Geophysical Research Letters

RESEARCH LETTER
10.1029/2020GL087667

Key Points:
- A new entraining cloud parcel model is developed to consider entrained aerosols
- A new critical entrainment rate is defined beyond which maximum supersaturation cannot be reached
- The results have important implications for considering entrainment mixing with entrained aerosols in droplet activation parameterization

Supporting Information:
- Supporting Information S1

Correspondence to:
J. Chen,
jingyi.chen@pnnl.gov

Citation:
Chen, J., Liu, Y., & Zhang, M. (2020). Effects of lateral entrainment mixing with entrained aerosols on cloud microphysics. *Geophysical Research Letters*, *47*, e2020GL087667. https://doi.org/10.1029/2020GL087667

Received 3 SEP 2019
Accepted 15 JUN 2020
Accepted article online 20 JUN 2020

©2020. American Geophysical Union. All Rights Reserved.

Effects of Lateral Entrainment Mixing With Entrained Aerosols on Cloud Microphysics

Jingyi Chen[1,2], Yangang Liu[1,3], and Minghua Zhang[1]

[1]School of Marine and Atmospheric Sciences, Stony Brook University, Stony Brook, NY, USA, [2]Pacific Northwest National Laboratory, Richland, WA, USA, [3]Brookhaven National Laboratory, Upton, NY, USA

Abstract The effects of entrained environment air and aerosols on cloud properties remain a critical yet understudied topic. This study first introduces a new entraining cloud parcel model considering entrained aerosols. With entrained aerosols represented by a newly introduced parameter, the impacts of entrainment rate and entrained aerosols on cloud microphysical properties are investigated. The results show that the relationships between entrainment rate and cloud microphysical properties are highly nonlinear when the entrained aerosols vary. With the lateral entrainment mixing, a new phenomenon is revealed that the height of maximum parcel supersaturation cannot be reached when the entrainment rate is beyond a certain critical value. This new critical entrainment rate is different from the critical entrainment rate defined by Barahona and Nenes (2007, https://doi.org/10.1029/2007JD008473), beyond which clouds cannot form. This finding has important implications for developing parameterization of droplet activation, which is based primarily on the assumption of the existence of maximum supersaturation.

Plain Language Summary In climate models, cloud droplet properties are calculated with simplified expressions (i.e., parameterizations), and cloud parcel models often serve as the benchmark model to develop such parameterizations; however, most studies are based on the adiabatic assumption that ignores entrainment of environmental air and aerosols. This study presents a new method to incorporate the effects of entrained air and aerosols into the cloud parcel model with little much increase of computational cost. The results reveal a new phenomenon that may have important implications for improving current parameterizations.

1. Introduction

Aerosol-cloud interactions are a critical factor determining cloud radiative properties, hydrological cycle, and the Earth energy budget (Albrecht, 1989; Lohmann & Feichter, 2005; Twomey, 1974, 1977). Based on global climate model simulations, aerosol properties and the mechanisms of aerosol-cloud interaction impact climate feedbacks and climate sensitivities through variations of cloud microphysical properties (Boucher et al., 2013; Donner et al., 2016; Levy et al., 2013; Rosenfeld, Sherwood, et al., 2014; Sherwood et al., 2014; Stainforth et al., 2005). Although aerosol-cloud interactions have been studied extensively, there are still significant discrepancies among different models and between models and observations (Chameides et al., 2002; Lohmann et al., 2010). Several plausible reasons have been proposed, including insufficient cloud physics theory (Liu et al., 2002), limited observations (Rosenfeld, Fischman, et al., 2014), and inadequate assumptions used in cloud parameterization schemes of large-scale models (e.g., droplet nucleation scheme; Chuang et al., 2012; Ghan et al., 2011; Zhao et al., 2016).

One of the widely used assumptions in parameterizations of cloud droplet nucleation and microphysics is the unrealistic adiabatic cloud (Ghan et al., 2011). This unrealistic assumption may be responsible for such outstanding problems as warm-rain initiation and spectral broadening (observational droplet size distributions are broader than those predicted by numerical models) (Beard & Ochs, 1993; Devenish et al., 2012; Telford, 1996). Nonadiabatic clouds have been studied by considering turbulent entrainment mixing over 70 years since Stommel (1947) described the fundamental hypothesis of mixing between ascending clouds and entrained dry air from surroundings. Numerical studies considering entrainment mixing following Stommel's idea include comparing with observations (Bewley & Lasher-Trapp, 2011; Jensen et al., 1985; Lee & Pruppacher, 1977; Mason & Chien, 1962; Su et al., 1998; Warner, 1973), theoretical understanding (Korolev et al., 2015; Pinsky et al., 2015; Yang et al., 2016), and development of new droplet activation schemes for climate models (Barahona & Nenes, 2007) (hereafter BN07).

Fractional entrainment rate (λ) is commonly used to characterize entrainment and the subsequent effects, and it impacts climate sensitivities in general circulation models (Sanderson et al., 2007). To examine the response of cloud droplet spectra to entrainment mixing, Lasher-trapp et al. (2005) performed an ensemble of cloud parcel model simulations with Lagrangian trajectories. Those trajectories were derived from cloud-resolving model simulations. They showed cloud droplet number concentration decreases due to either dilution by entraining droplet-free air (equation 7 in Lasher-trapp et al., 2005) or highly inhomogeneous mixing degree (equation 9 in Lasher-trapp et al., 2005). Subsequently, the considerable growth of the remaining active cloud particles is stimulated. The condensation on those large cloud droplets dominates over the droplet evaporation due to decreased supersaturation by entrained dry air, broadening droplet size distributions toward the large size. Yang et al. (2016) investigated the homogeneous mixing scenario by deriving analytical expressions for the "superadiabatic" growth after single entrainment event. Most of the previous studies have been primarily focused on understanding the role of decreasing supersaturation due to entrainment mixing in affecting cloud droplet size distributions.

Entrainment can bring aerosol particles or cloud condensation nuclei (CCN) into clouds and thus affect cloud microphysical properties as well. For example, Lasher-trapp et al. (2005) showed that entrained CCN trigger more competition among cloud droplets, broaden cloud droplet size distributions toward smaller sizes, and decrease the droplet size. However, the treatment of entrained aerosols often assumes that entrained aerosols are a certain fraction of aerosols at cloud base, although it has been known that considerable amount of the entrained air is not originated from cloud base (Jensen et al., 1985; Lasher-trapp et al., 2005; Paluch, 1979). Even though there are reasons for using this overly simplified treatment (e.g., insufficient aerosol measurements along cloud edges and computational cost/feasibility to continually entrained CCN; Lasher-trapp et al., 2005; Warner, 1973), inadequate treatment of the impacts from various entrained aerosols may cause misinterpretation of entrainment mixing, inaccurate evaluations of aerosol-cloud interactions on climate, and large uncertainties in numerical simulations.

Still understudied is to represent the effect of entrainment on droplet activation for climate models. To the best of our knowledge, BN07 is the only work that has been done in this regard. They developed a parameterization for large-scale models based on the newly defined critical entrainment rate and "population splitting" approach (Nenes & Seinfeld, 2003). The parameterization first determines if any particle of the CCN population is able to activate by comparing the entrainment rate with the critical entrainment rate. If the entrainment rate is smaller than the critical entrainment rate, the maximum supersaturation and cloud droplet number concentration are calculated analytically by "population splitting" approach, which divides CCN into two groups with one has low critical supersaturation and substantial growth after activation and the remaining another one. However, the BN07 parameterization does not consider the effects of entrained aerosols.

Thus, the objectives of this study are to first extend our adiabatic parcel model (Chen et al., 2016, 2018) to consider entrainment of both environmental air and aerosols and then to explore the impacts of entrainment and entrained aerosols on cloud microphysical properties and aerosol-cloud interactions by this new model. In particular, it is shown that there exists another critical entrainment rate beyond which the parcel supersaturation continues to increase with increasing heights without reaching a maximum. This new finding raises questions as to the assumption of the existence of maximum supersaturation on which virtually all the droplet activation parameterizations are based, including the BN07 parameterization, and presents new challenges to develop general parameterizations of aerosol-cloud interactions in climate models.

2. Description of Entraining Cloud Parcel Model

The cloud parcel model used in this study is built on the adiabatic version (Chen et al., 2016, 2018) in which updraft cooling causes supersaturation in the cloud parcel, stimulating water vapor condensing on the aerosols and existing cloud droplets. The vapor diffusion process is described by the condensational growth equation (Lamb & Verlinde, 2011). The κ-Köhler model is used to treat aerosol hygroscopic growth and droplet activation (Petters & Kreidenweis, 2007; Pöschl et al., 2010). The numerical scheme follows the ordinary differential equation solver released in 2013 in Fortran 90 (VODE-F90), which is an extension of the

well-known VODE (Brown et al., 1989), and improves the model performance. Particles are represented by the Lagrangian particle size bins. The treatment of entrainment mixing is briefly described below; detailed derivation is given in the supporting information.

The particle number concentration is described by

$$\frac{\mathrm{d}N_{am}}{\mathrm{d}t} = -\lambda\, wN_{am} + \lambda wN_{am,e}, \tag{1}$$

where N_{am} is the total particle number concentration per unit mass of air, t is the time, λ is the fractional entrainment rate, w is the vertical velocity of the parcel, and the subscript "e" indicates that the quantity is for the one from the environmental air. The first and second terms on the right-hand side (RHS) of Equation 1 are the dilution of the number concentration due to the entrainment mixing and the entrained aerosols, respectively. A key aspect of the new model is related to the treatment of the second term. Without loss of generality, we introduce a dimensionless parameter α_i defined as the ratio of the particle concentration of the ith bin from the environment air to the in-cloud particle concentration given by

$$\alpha_i = \frac{N_{ami,e}}{N_{ami}}. \tag{2}$$

In principle, α_i takes on different values for different sized particles to consider the effect of particle size on entrained aerosols. However, this detailed treatment requires tracking α_i for all the size bins, which is computationally prohibitive for use in climate models. In the spirit of simplifying the treatment of entrained aerosols for developing droplet activation parameterization in climate models, we further assume that the effect of entrained aerosols can be represented by a single value of α, that is, $\alpha_i = \alpha$. Thus, we have

$$\alpha = \frac{N_{am,e}}{N_{am}}, \tag{3}$$

where the newly introduced parameter α denotes the entrained fraction of total number concentration for all the particles. Two special scenarios are noteworthy: when $\alpha = 0$, entrained aerosols are not considered, and change of particle concentration resulting from entrainment mixing is due fully to the dilution caused by entrained dry air. When $\alpha = 1$, effect of entrained aerosols balances the particle dilution, and hence, the total particle number concentration does not change. The latter scenario is implicitly assumed in BN07. It should be emphasized that the model with this assumption is a generalization of existing models and is a focus of this study. The more general set of equations and the relationship between α and α_i are provided in the supporting information.

Water vapor mixing ratio and liquid water mixing ratio are described by Equations 4 and 5, respectively:

$$\frac{\mathrm{d}q_v}{\mathrm{d}t} = -\left(\frac{\mathrm{d}q_l}{\mathrm{d}t}\right)_{cd} - \lambda\, w\left(q_v - q_{v,e}\right) - \lambda \mathrm{w}\alpha q_l, \tag{4}$$

$$\frac{\mathrm{d}q_l}{\mathrm{d}t} = \left(\frac{\mathrm{d}q_l}{\mathrm{d}t}\right)_{cd} - \lambda w q_l + \lambda w \alpha q_l, \tag{5}$$

where q_l is the liquid water mixing ratio and q_v is the water vapor mixing ratio. The first terms on the RHS of Equations 4 and 5 describe the condensation or evaporation of the particles in the original parcel, and the rest of the terms describe the effects of entrainment mixing. The second and third terms on the RHS of Equation 4 describe the dilution of water vapor and the sink from condensation on the entrained aerosols, respectively. The second and third terms of Equation 5 describe the dilution of liquid water and the source from condensation on entrained aerosols, respectively. See Equations S2 and S5 wherein the generalized

form of Equations 4 and 5 is given based on the definition of liquid water mixing ratio and conservation law. The term $\left(\frac{dq_l}{dt}\right)_{cd}$ is calculated by the diffusional growth equation given by

$$\left(\frac{dq_l}{dt}\right)_{cd} = \frac{\rho_a}{\rho_d}\sum_i \left(N_{am,i}\frac{dm_i}{dt}\right), \tag{6a}$$

$$\frac{dm_i}{dt} = \frac{4\pi r_i\left(S_p - S_{k,i}\right)}{\dfrac{RT}{M_w\, D'_v\, e_s(T)} + \dfrac{l_v}{\left(M_w\, k'_T\, T\right)\left(\dfrac{l_v}{RT} - 1\right)S_{k.i}}}, \tag{6b}$$

where r is the particle radius, S_p is the parcel supersaturation, S_k is the particle equilibrium supersaturation, T is the air temperature, M_w is the mole mass of water, ρ_w is the water density, e_s is the saturation water vapor pressure, l_v is the latent heat, and D'_v and k'_T are the modified diffusion coefficient and thermal conductivity, respectively, including near droplet surface modification (Lamb & Verlinde, 2011). The summation on the RHS of Equation 6a applies to all wet particles in the cloud parcel (not to the entrained particles). The condensation of water vapor on entrained particles is represented by the third term of Equation 5 ignoring the kinetic growth by vapor diffusion.

The air parcel temperature is influenced by the mixing of specific heat between the parcel and environment air and the latent heat from the condensation and evaporation on both original and entrained particles. Thus, the change of temperature is derived by modifying the adiabatic version based on the energy conservation:

$$\frac{dT}{dt} = -\frac{gw}{c_p} + \frac{l_v}{c_p}\left[\left(\frac{dq_l}{dt}\right)_{cd} + \lambda w \alpha q_l\right] - \lambda\, w\, (T - T_e), \tag{7}$$

where g is the gravity acceleration and c_p is the heat capacity of moist air. On the RHS of Equation 7, the three terms represent the dry adiabatic cooling, latent heat from water phase change between liquid and water vapor, and the mixing of specific heat between upward air parcel and environmental air. Note that the second term has two contributions: one from the original particles in the air parcel and the other from entrained particles.

Together with the time tendency of air pressure with the assumption of hydrostatic balance, these equations constitute the closed set of equations for the new entraining cloud parcel model that accounts explicitly for the effects of entrained aerosols through the parameter α. The values of the coefficients and constants are the same as Chen (2018). This model provides a computationally efficient way to implement entrained aerosols into the Lagrangian cloud parcel model.

3. Results

BN07 presented the first cloud droplet activation parameterization that considers the entrainment of dry air. Briefly, the BN07 parameterization used the "population splitting" method (Nenes & Seinfeld, 2003) to obtain maximum supersaturation ($S_{\max}$) and cloud droplet number concentration. Effects of entraining dry air into the cloud parcel are parameterized into the calculation of $S_{\max}$ by computing the conservation of energy and water vapor for an unsaturated entraining parcel. Also, the importance of lateral entrainment is considered by defining the critical entrainment rate, beyond which no aerosol particles can be activated into cloud droplets because the $S_{\max}$ is below 0 (hereafter the first critical entrainment rate and denoted by λ_{c1}).

The BN07 parameterization was developed in terms of the modified $S_{\max}$ calculation and the first critical entrainment rate. However, the BN07 droplet activation does not consider the effect of entrained aerosols,

leaving an area for further exploration. Based on the theoretical framework described in section 3, we can derive the time tendency equation of S_p given by

$$\frac{\mathrm{d}S_p}{\mathrm{d}t} = aw - b\left[\left(\frac{\mathrm{d}q_l}{\mathrm{d}t}\right)_{cd} + \lambda\, w\alpha\, q_l\right] + \lambda\, w\left[\frac{l_v(1+S_p)}{R_vT^2}(T-T_e) - \frac{PM_d}{e_sM_w}\left(q_v - q_{v,e}\right)\right], \tag{8a}$$

$$a = (1+S_p)\left(\frac{gl_v}{R_vc_pT^2} - \frac{g}{R_aT}\right), \tag{8b}$$

$$b = \frac{(1+S_p)l_v^2}{c_pR_vT^2} + \frac{PM_d}{e_sM_w}. \tag{8c}$$

Note that Equations 8a–8c is not the equation numerically solved in the model; it is derived from Equations 4 and 7 to help understand the behavior of supersaturation. A comparison of Equations 8a–8c with the corresponding equation in BN07 (i.e., Equations 8a–8c) reveals that the major difference between the two equations lies in the second term. Our Equations 8a–8c reduces to that in BN07 when $\alpha = 1$. Thus, our new equation is essentially a first-order generalization of the BN07 equation to consider the effects of entrained aerosols through the parameter of α.

3.1. Impacts of Lateral Entrainment Mixing on Cloud Microphysics

To examine the effects of λ and α, we conduct a suite of numerical simulations with wide ranges of λ (0–6.4 km^{-1} with 0.1 as interval) and α (0–2 with 0.5 as interval) under a variety of combined conditions of initial aerosol concentration per unit volume (N_a) and updraft velocity (w). Briefly, the initial aerosols are assumed to follow lognormal size distributions with fixed geometrical mean radius of 0.06 μm and geometrical deviation of 1.5. The aerosol composition is assumed to be sulfate ammonium with hygroscopicity parameter as 6.1. Initial air temperature, air pressure, and relative humidity are 283.15 K, 919 hPa, and 95%, respectively. Entrained dry air is 1 K lower than the cloudy parcel and has relative humidity as 85%. The values of N_a and w are specified in the text below.

According to the adiabatic theory ($\lambda = 0$), S_p first increases with increasing heights due to updraft cooling (the first term of Equations 8a–8c), peaks at a certain height, and then decreases with further parcel rising because the sink term of the condensation processes starts to dominate (the second term of Equations 8a–8c). The peak point corresponds to the $S_{\max}$ whereby the production from updraft cooling is balanced by the consumption from condensation. This classical picture of S_p serves as the foundation of virtually all the droplet activation parameterizations (Ghan et al., 2011).

Consideration of entrainment and especially entrained aerosols makes the behavior of S_p more complicated than this classical picture. Figure 1 shows the vertical profiles of S_p at four different values of λ and five different values of α. The value of N_a is 1,000 cm^{-3}, and w is 2 m s^{-1}. When $\alpha \geq 1$ (Figures 1c–1e), the behaviors of S_p are similar to the classical picture and that described by BN07, and an increase in λ does not change the fundamental pattern of S_p varying with height but leads to an increase in the peak height and a decrease of $S_{\max}$. When $\lambda > \lambda_{c1}$, the values of $S_{\max}$ are smaller than 0, and thus, no aerosol particles can be activated into cloud droplets (e.g., the green lines in Figures 1e, 2e, and 3e). However, when $\alpha < 1$, the behaviors of S_p become different from the classical picture; after λ reaching certain value, S_p keeps on increasing monotonically with increasing height, without reaching a peak $S_{\max}$ (e.g., the green line in Figure 1a).

To physically understand the results, Figures 2a–2e and 3 show the vertical profiles of cloud droplet number concentration per dry air mass (N_{cm}) and liquid water content (LWC), respectively, for the same cases as Figure 1 shows. Here cloud droplet number concentration is shown in the unit of per mass to avoid the impact of air density change on number concentration per volume. Without entrained aerosols or with less entrained aerosols ($\alpha < 1$), N_{cm} decreases with height significantly after reaching the peak value due to the dilution of the cloudy parcel by entrained environmental air with fewer entrained particles. As λ increases, the dilution effect becomes stronger and results in an overall negative relationship between N_{cm} and λ. The small amount of cloud condensates causes a weak condensation sink for S_p and results in the monotonically

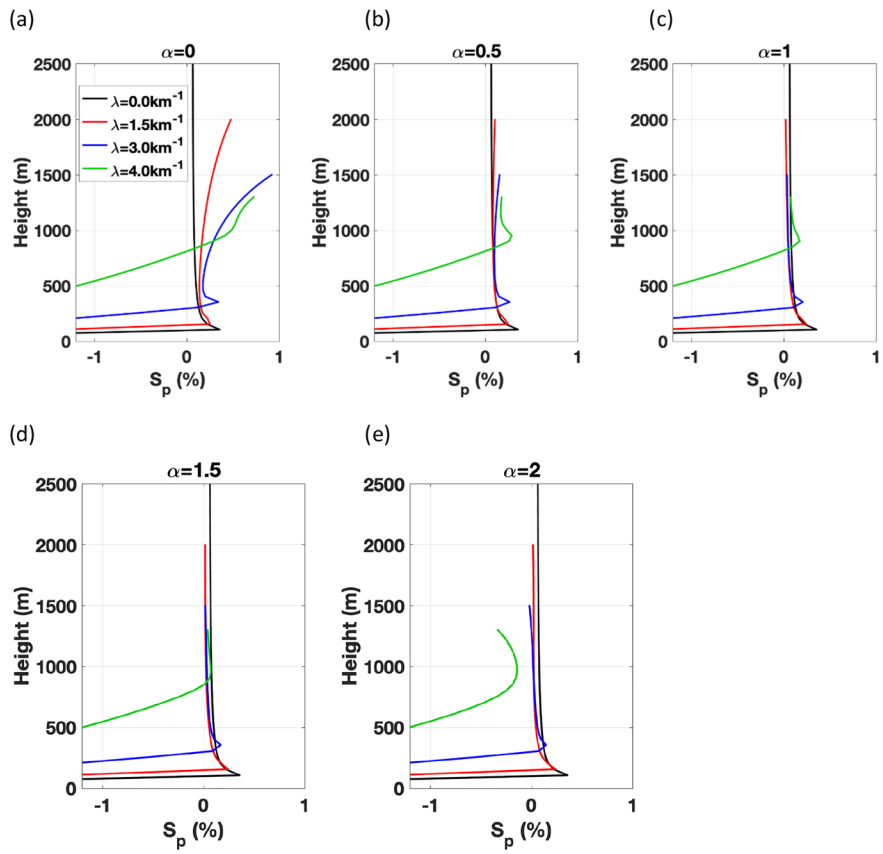

Figure 1. Vertical profiles of parcel supersaturation (S_p) at various values of entrainment rate (λ) with (a) entrained aerosol parameter $\alpha = 0$, (b) $\alpha = 0.5$, (c) $\alpha = 1.0$, (d) $\alpha = 1.5$, and (e) $\alpha = 2$. The simulations are for $N_a = 1{,}000$ cm^{-3} and $w = 2$ m s^{-1}.

increasing S_p with height. On the other hand, when $\alpha \geq 1$, the dilution effect on droplet concentration is negated by the entrained aerosols, making the condensation term strong enough to deplete water vapor and decrease S_p as the parcel rises like for the adiabatic parcel model. Figure 3 shows that an increase of λ reduces LWC as expected; but variation of α has little impacts on LWC. A comparative analysis of Figures 2 and 3 shows that the consideration of α mainly affects the redistribution of LWC among cloud droplets at different droplet sizes, without influence on the total amount of condensed cloud water.

The impacts of increasing S_p with height on cloud droplet concentration are shown in Figure 2f by the vertical profiles of the differences between N_{cm} at $\alpha = 0$ (without entrained aerosols) and the $N_{cm,\text{dilute}}$ (only considering dilution effect) from

$$\frac{\mathrm{d}N_{cm,\text{dilute}}}{\mathrm{d}t} = -\lambda w N_{cm}. \tag{9}$$

When $\alpha = 0$, N_{cm} is determined only by two mechanisms: new activation/deactivation and dilution. Thus, a positive difference shown in Figure 2f suggests some new particle activation due to the monotonic increasing of S_p. It is interesting to note that the increase of S_p is continuous whereas new particle activation is discrete, because new aerosols are activated only when S_p reaches the critical supersaturation of the largest inactivated aerosol.

3.2. Two Critical Entrainment Rates

The preceding results suggest that under certain conditions, a new critical entrainment rate exists beyond which S_p increases monotonically with height without reaching $S_{\max}$. We define it as the second critical

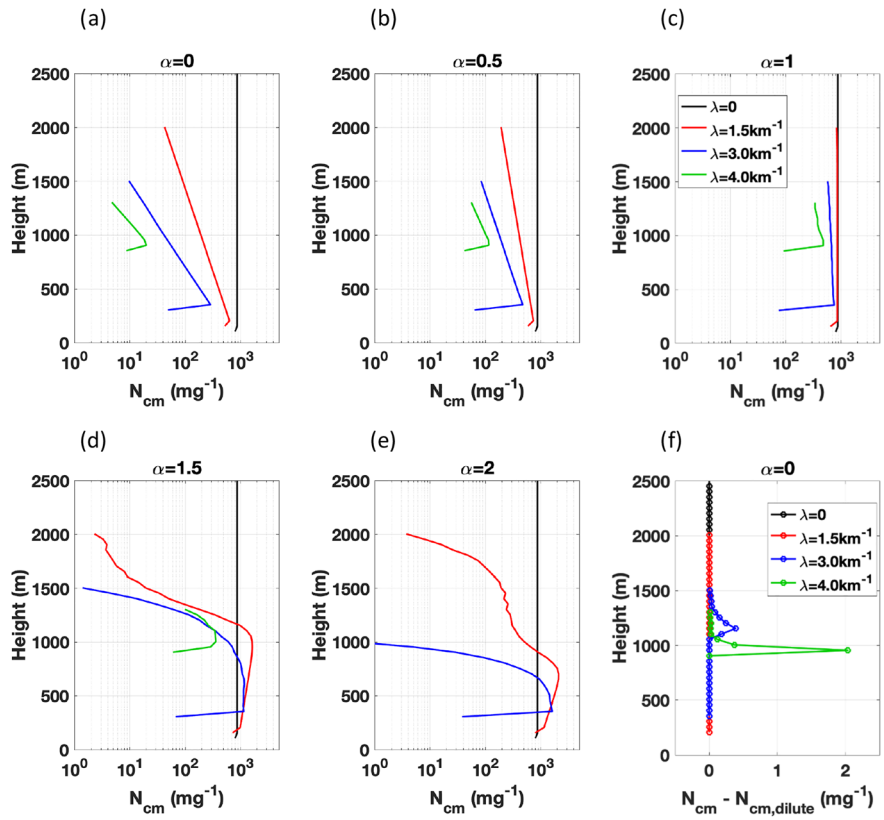

Figure 2. Vertical profiles of cloud droplet number concentration (N_{cm}) per unit mass of moist air at various values of entrainment rate (λ) with (a) entrained aerosol parameter $\alpha = 0$, (b) $\alpha = 0.5$, (c) $\alpha = 1.0$, (d) $\alpha = 1.5$, and (e) $\alpha = 2$. (f) Vertical profiles of the differences between N_{cm} and $N_{cm,\mathrm{dilute}}$ when $\alpha = 0$. See text for more details.

entrainment rate and denote it by λ_{c2}, in distinction with the first critical entrainment rate defined in BN07 (λ_{c1}). The presence of λ_{c2} has crucial implications for understanding cloud properties in general and for developing parameterization of droplet activation in particular, since the existence of $S_{\max}$ serves as the basis for virtually all droplet activation parameterizations.

Furthermore, the results shown in section 3.1 are for the case of $N_a = 1{,}000\ \mathrm{cm}^{-3}$ and $w = 2\ \mathrm{m\ s}^{-1}$. The behaviors of the two critical entrainment rates likely depend on different combinations of N_a and w or different aerosol-cloud interaction regimes as discussed in our previous studies (Chen et al., 2016, 2018). Figures S1–S6 show profiles of S_p, N_{cm}, and LWC similar to Figures 1–3 except for different values of N_a and w. Thus, we further examine the dependence of λ_{c1} and λ_{c2} on α under different combinations of N_a and w (Figure 4). Five values of N_a (100, 500, 800, 1,000, and 10,000 cm^{-3}) and four values of w (0.1, 1, 2, and 5 $\mathrm{m\ s}^{-1}$) are used for Figure 4. Figure 4a shows that λ_{c1} does not depend on the values of α when $\alpha < 1$, but λ_{c2} increases with α. It can be understood that a higher value of α (more entrained aerosols) leads to a stronger depletion of water vapor, smaller S_p, and larger λ_{c2} is needed to cause increasing S_p with height. Also, Figure 4b shows that a larger N_a/w causes a larger λ_{c2} when $\alpha \leq 1$. This is because a higher N_a enhances water vapor depletion; a smaller w diminishes available water vapor, delaying λ_{c2} to a higher value.

Besides, when $\alpha \leq 1$ and N_a/w is not too large, the values of λ_{c2} are smaller than λ_{c1} and gradually approach λ_{c1} as α increases. This means that before the droplet activation is prohibited ($\lambda < \lambda_{c1}$), there is a zone that $S_{\max}$ cannot be found. However, when α is much larger than 1, λ_{c2} is larger than λ_{c1}, especially with high values of N_a/w, suggesting that the sink term of supersaturation is strong enough so that $S_{\max}$ is reached even when S_p is less than 0. This condition requires a large number of water-soluble aerosols. When

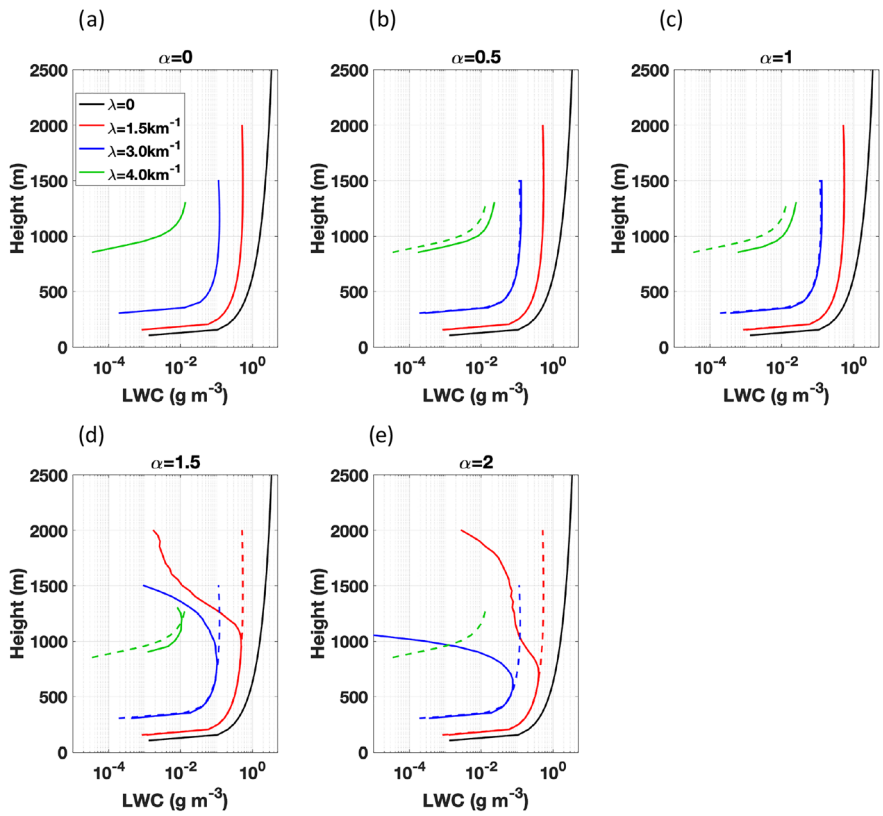

Figure 3. Vertical profiles of liquid water content (LWC) at various values of entrainment rate (λ) with (a) entrained aerosol parameter $\alpha = 0$, (b) $\alpha = 0.5$, (c) $\alpha = 1.0$, (d) $\alpha = 1.5$, and (e) $\alpha = 2$. The dashed lines in (b)–(e) are the same as the solid lines in the corresponding colors except for $\alpha = 0$.

$\alpha < 1$, a small number of wet aerosols do not absorb water vapor fast enough to enable the source term (updraft cooling term, the first term on RHS of Equations 8a–8c) to dominate, and λ_{c2} is not larger than λ_{c1} before S_p is larger than 0.

Furthermore, Figure 4a shows that λ_{c1} decreases with α when N_a/w is high and/or $\alpha > 1$, suggesting that a large number of cloud condensates, either from cloud base or through lateral entrainment mixing, cause too much water vapor depletion before S_p reaches 0 and prohibit the formation of cloud droplets.

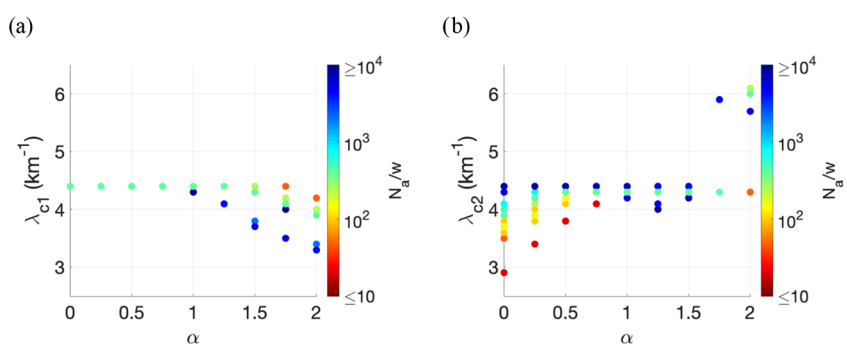

Figure 4. Dependence of the first (a) and second (b) critical entrainment rates on the entrained aerosol parameter α. The color scheme denotes the regime of aerosol-cloud interactions as measured by the ratio of initial aerosol concentration N_a to the updraft velocity w.

4. Concluding Remarks

A novel entraining cloud parcel model is developed that accounts explicitly for not only entrained environmental air but also entrained aerosols by extending our adiabatic cloud parcel model introduced in Chen et al. (2016, 2018). A new dimensionless parameter α is introduced to quantify the strength and effects of entrained aerosols. New time tendency equations for water mixing ratio and number concentration are derived to explicitly include α. The new equations provide a computational efficient way to examine the effects of entrained aerosols on droplet activation and cloud microphysical properties.

A new phenomenon is found that under certain conditions, parcel supersaturation increases monotonically with increasing heights without reaching its maximum as normally assumed, as a result of strong dilution caused by entrainment of environment air and insufficient supply of entrained aerosols during entrainment-mixing processes. New activation of small cloud droplets is the subsequent result of the monotonic increasing of parcel supersaturation. Accordingly, a new critical entrainment rate (λ_{c2}) is defined, beyond which the maximum supersaturation cannot be reached. This newly defined critical entrainment rate is compared with that proposed in BN07 (λ_{c1}). The dependences of both λ_{c1} and λ_{c2} on α, aerosol concentration, and vertical velocities are discussed.

Several points are noteworthy. First, the existence of λ_{c2} has crucial implications for developing droplet activation parameterization. It is shown that before reaching the maximum S_p, a combination of rising S_p and entrained aerosols causes additional droplet activation. The additional activation alters cloud properties and likely broadens the cloud droplet size distribution. However, existing parameterizations are all based on the assumption of existence of maximum S_p and thus do not represent such conditions. Second, the new model is built on the assumption that α is independent of particle sizes or the entrained particles only change the number concentration. This assumption needs to be evaluated and relaxed in the future work. Third, it is desirable to have analytical expressions for the two critical entrainment rates, which are discussed in the supporting information. Finally, the findings are based on our modeling study; observational study is needed to confirm and substantiate them.

Data Availability Statement

The simulation data in this study have been uploaded in repository "fig share" (https://doi.org/10.6084/m9.figshare.9744857.v1).

Acknowledgments

This study is supported by the U.S. Department of Energy Office of Science Biological and Environmental Research as part of the Atmospheric Systems Research (ASR) Program. Brookhaven National Laboratory and Pacific Northwest National Laboratory are operated by Battelle for the U.S. Department of Energy under Contracts DE-SC0012704 and DE-AC05-76RLO1830, respectively.

References

Albrecht, B. A. (1989). Aerosols, cloud microphysics, and fractional cloudiness. *Science*, *245*(4923), 1227–1230. https://doi.org/10.1126/science.245.4923.1227

Barahona, D., & Nenes, A. (2007). Parameterization of cloud droplet formation in large-scale models: Including effects of entrainment. *Journal of Geophysical Research*, *112*, D16206. https://doi.org/10.1029/2007JD008473

Beard, K. V., & Ochs, H. T. (1993). Warm-rain initiation: An overview of microphysical mechanisms. *Journal of Applied Meteorology*, *32*(4), 608–625. https://doi.org/10.1175/1520-0450(1993)032%3C0608:WRIAOO%3E2.0.CO;2

Bewley, J. L., & Lasher-Trapp, S. (2011). Progress on predicting the breadth of droplet size distributions observed in small cumuli. *Journal of the Atmospheric Sciences*, *68*(12), 2921–2929. https://doi.org/10.1175/JAS-D-11-0153.1

Boucher, O., Randall, D., Artaxo, P., Bretherton, C., Feingold, G., Forster, P., et al. (2013). Clouds and aerosols. In: Climate change 2013: The physical science basis. In *Contribution of Working Group I to the Fifth Assessment Report of the Intergovernmental Panel on Climate Change*. Cambridge, United Kingdom and New York, NY, USA: Cambridge University Press.

Brown, P. N., Byrne, G. D., & Hindmarsh, A. C. (1989). VODE: A variable-coefficient ODE solver. *SIAM Journal on Scientific and Statistical Computing*, *10*(5), 1038–1051. https://doi.org/10.1137/0910062

Chameides, W. L., Luo, C., Saylor, R., Streets, D., Huang, Y., Bergin, M., & Giorgi, F. (2002). Correlation between model-calculated anthropogenic aerosols and satellite-derived cloud optical depths: Indication of indirect effect? *Journal of Geophysical Research*, *107*(D10), 4085. https://doi.org/10.1029/2000JD000208

Chen, J., Liu, Y., Zhang, M., & Peng, Y. (2016). New understanding and quantification of the regime dependence of aerosol-cloud interaction for studying aerosol indirect effects. *Geophysical Research Letters*, *43*, 1780–1787. https://doi.org/10.1002/2016GL067683

Chen, J. (2018). *Investigation and parameterization of aerosol-cloud interactions using cloud parcel model and observations* (Chap. 2, pp. 5–9). Stony Brook University.

Chen, J., Liu, Y., Zhang, M., & Peng, Y. (2018). Height dependency of aerosol-cloud interaction regimes. *Journal of Geophysical Research: Atmospheres*, *123*, 491–506. https://doi.org/10.1002/2017JD027431

Chuang, C. C., Kelly, J. T., Boyle, J. S., & Xie, S. (2012). Sensitivity of aerosol indirect effects to cloud nucleation and autoconversion parameterizations in short-range weather forecasts during the May 2003 aerosol IOP. *Journal of Advances in Modeling Earth Systems*, *4*, M09001. https://doi.org/10.1029/2012MS000161

Devenish, B. J., Bartello, P., Brenguier, J. L., Collins, L. R., Grabowski, W. W., IJzermans, R. H. A., et al. (2012). Droplet growth in warm turbulent clouds. *Quarterly Journal of the Royal Meteorological Society*, *138*(667), 1401–1429. https://doi.org/10.1002/qj.1897

Donner, L. J., O'Brien, T. A., Rieger, D., Vogel, B., & Cooke, W. F. (2016). Are atmospheric updrafts a key to unlocking climate forcing and sensitivity? *Atmospheric Chemistry and Physics*, *16*(20), 12,983–12,992. https://doi.org/10.5194/acp-16-12983-2016

Ghan, S. J., Abdul-Razzak, H., Nenes, A., Ming, Y., Liu, X., Ovchinnikov, M., et al. (2011). Droplet nucleation: Physically-based parameterizations and comparative evaluation. *Journal of Advances in Modeling Earth Systems*, *3*, M10001. https://doi.org/10.1029/2011MS000074

Jensen, J. B., Austin, P. H., Baker, M. B., & Blyth, A. M. (1985). Turbulent mixing, spectral evolution and dynamics in a warm cumulus cloud. *Journal of the Atmospheric Sciences*, *42*(2), 173–192. https://doi.org/10.1175/1520-0469(1985)042%3C0173:TMSEAD%3E2.0.CO;2

Korolev, A., Khain, A., Pinsky, M., & French, J. (2015). Theoretical study of mixing in liquid clouds—Part 1: Classical concept. *Atmospheric Chemistry and Physics Discussions*, *15*(21), 30,211–30,267. https://doi.org/10.5194/acpd-15-30211-2015

Lamb, D., & Verlinde, J. (2011). Growth from the vapor. *In Physics and chemistry of clouds* (pp. 320–279). New York: Cambridge University Press. https://doi.org/10.1017/CBO9780511976377

Lasher-trapp, S. G., Cooper, W. A., & Blyth, A. M. (2005). Broadening of droplet size distributions from entrainment and mixing in a cumulus cloud. *Quarterly Journal of the Royal Meteorological Society*, *131*(605), 195–220. https://doi.org/10.1256/qj.03.199

Lee, I.-Y., & Pruppacher, H. R. (1977). A comparative study on the growth of cloud drops by condensation using an air parcel model with and without entrainment. *pure and applied geophysics*, *115*(3), 523–545. https://doi.org/10.1007/BF00876119

Levy, H., Horowitz, L. W., Schwarzkopf, M. D., Ming, Y., Golaz, J.-C., Naik, V., & Ramaswamy, V. (2013). The roles of aerosol direct and indirect effects in past and future climate change. *Journal of Geophysical Research: Atmospheres*, *118*, 4521–4532. https://doi.org/10.1002/jgrd.50192

Liu, Y., Daum, P. H., Chai, S., & Liu, F. (2002). Cloud parameterizations, cloud physics and their connections: An overview. *Recent Research Developments in Geophysics*, *4*, 119–142.

Lohmann, U., & Feichter, J. (2005). Global indirect aerosol effects: A review. *Atmospheric Chemistry and Physics*, *5*(3), 715–737. https://doi.org/10.5194/acp-5-715-2005

Lohmann, U., Rotstayn, L., Storelvmo, T., Jones, A., Menon, S., Quaas, J., et al. (2010). Total aerosol effect: Radiative forcing or radiative flux perturbation? *Atmospheric Chemistry and Physics*, *10*(7), 3235–3246. https://doi.org/10.5194/acp-10-3235-2010

Mason, B. J., & Chien, C. W. (1962). Cloud-droplet growth by condensation in cumulus. *Quarterly Journal of the Royal Meteorological Society*, *88*(376), 136–142. https://doi.org/10.1002/qj.49708837603

Nenes, A., & Seinfeld, J. H. (2003). Parameterization of cloud droplet formation in global climate models. *Journal of Geophysical Research*, *108*(D14), 4415. https://doi.org/10.1029/2002JD002911

Paluch, I. R. (1979). The entrainment mechanism in Colorado cumuli. *Journal of the Atmospheric Sciences*, *36*(12), 2467–2478. https://doi.org/10.1175/1520-0469(1979)036%3C2467:TEMICC%3E2.0.CO;2

Petters, M. D., & Kreidenweis, S. M. (2007). A single parameter representation of hygroscopic growth and cloud condensation nucleus activity. *Atmospheric Chemistry and Physics*, *7*(8), 1961–1971. https://doi.org/10.5194/acp-7-1961-2007

Pinsky, M., Khain, A., Korolev, A., & Magaritz-Ronen, L. (2015). Theoretical investigation of mixing in warm clouds—Part 2: Homogeneous mixing. *Atmospheric Chemistry and Physics Discussions*, *15*(21), 30,269–30,320. https://doi.org/10.5194/acpd-15-30269-2015

Pöschl, U., Martin, S. T., Sinha, B., Chen, Q., Gunthe, S. S., Huffman, J. A., et al. (2010). Rainforest aerosols as biogenic nuclei of clouds and precipitation in the Amazon. *Science*, *329*(5998), 1513–1516. https://doi.org/10.1126/science.1191056

Rosenfeld, D., Fischman, B., Zheng, Y., Goren, T., & Giguzin, D. (2014). Combined satellite and radar retrievals of drop concentration and CCN at convective cloud base. *Geophysical Research Letters*, *41*, 3259–3265. https://doi.org/10.1002/2014GL059453

Rosenfeld, D., Sherwood, S., Wood, R., & Donner, L. (2014). Climate effects of aerosol-cloud interactions. *Science*, *343*(6169), 379–380. https://doi.org/10.1126/science.1247490

Sanderson, B. M., Piani, C., Ingram, W. J., Stone, D. A., & Allen, M. R. (2007). Towards constraining climate sensitivity by linear analysis of feedback patterns in thousands of perturbed-physics GCM simulations. *Climate Dynamics*, *30*(2-3), 175–190. https://doi.org/10.1007/s00382-007-0280-7

Sherwood, S. C., Bony, S., & Dufresne, J.-L. (2014). Spread in model climate sensitivity traced to atmospheric convective mixing. *Nature*, *505*(7481), 37–42. https://doi.org/10.1038/nature12829

Stainforth, D. A., Aina, T., Christensen, C., Collins, M., Faull, N., Frame, D. J., et al. (2005). Uncertainty in predictions of the climate response to rising levels of greenhouse gases. *Nature*, *433*(7024), 403–406. http://www.nature.com/nature/journal/v433/n7024/suppinfo/nature03301_S1.html, https://doi.org/10.1038/nature03301

Stommel, H. (1947). Entrainment of air into a cumulus cloud. *Journal of Meteorology*, *4*(3), 91–94. https://doi.org/10.1175/1520-0469(1947)004%3C0091:EOAIAC%3E2.0.CO;2

Su, C.-W., Krueger, S. K., McMurtry, P. A., & Austin, P. H. (1998). Linear eddy modeling of droplet spectral evolution during entrainment and mixing in cumulus clouds. *Atmospheric Research*, *47-48*, 41–58. https://doi.org/10.1016/S0169-8095(98)00039-8

Telford, J. W. (1996). Clouds with turbulence; the role of entrainment. *Atmospheric Research*, *40*(2–4), 261–282. https://doi.org/10.1016/0169-8095(95)00038-0

Twomey, S. (1974). Pollution and the planetary albedo. *Atmospheric Environment (1967)*, *8*(12), 1251–1256. https://doi.org/10.1016/0004-6981(74)90004-3

Twomey, S. (1977). The influence of pollution on the shortwave albedo of clouds. *Journal of the Atmospheric Sciences*, *34*(7), 1149–1152. https://doi.org/10.1175/1520-0469(1977)034%3C1149:TIOPOT%3E2.0.CO;2

Warner, J. (1973). The microstructure of cumulus cloud: Part IV. The effect on the droplet spectrum of mixing between cloud and environment. *Journal of the Atmospheric Sciences*, *30*(2), 256–261. https://doi.org/10.1175/1520-0469(1973)030%3C0256:TMOCCP%3E2.0.CO;2

Yang, F., Shaw, R., & Xue, H. (2016). Conditions for super-adiabatic droplet growth after entrainment mixing. *Atmospheric Chemistry and Physics Discussions*, *2016*, 1–24. https://doi.org/10.5194/acp-2016-94

Zhao, M., Golaz, J. C., Held, I. M., Ramaswamy, V., Lin, S. J., Ming, Y., et al. (2016). Uncertainty in model climate sensitivity traced to representations of cumulus precipitation microphysics. *Journal of Climate*, *29*(2), 543–560. https://doi.org/10.1175/JCLI-D-15-0191.1